Model Experiment on Parametric Rolling of a Post-Panamax Containership in Head Waves

Harukuni Taguchi, *National Maritime Research Institute (NMRI)*

Shigesuke Ishida, *National Maritime Research Institute (NMRI)*

Hiroshi Sawada, *National Maritime Research Institute (NMRI)*

Makiko Minami, *National Maritime Research Institute (NMRI)*

ABSTRACT

Parametric rolling resonance in head waves was investigated experimentally. An experiment using a scale model of a post-Panamax containership was carried out in regular head waves at the 80 metres square basin of NMRI. In the experiment the wavelength, the wave height, the model speed and the encounter angle were widely varied to clarify overall property of parametric rolling resonance in head waves. As a result, conditions in which the head wave parametric rolling resonance is likely to occur and effects of the encounter period, the wave height and the encounter angle on parametric rolling amplitude were clarified. Moreover numerical simulations of roll motion of a ship in pure head waves were also carried out to investigate the property of parametric rolling resonance further.

Keywords: *parametric rolling in head waves, post-Panamax containership, International Maritime Organization, Intact Stability Code*

1. INTRODUCTION

A post-Panamax containership accident in the north Pacific Ocean, in which that ship suffered extensive loss and damage to onboard containers due to severe parametric rolling in head wave condition (France et al., 2003), led the International Maritime Organization (IMO) to start work to revise the Intact Stability Code (IS Code) in this aspect.

Regarding parametric rolling resonance, phenomenon in following waves is well known, while that in head waves has been less studied so far (e.g. Dallinga et al., 1998, Neves and Valerio, 2000, France et al., 2003, Neves et al., 2003, Bulian et al., 2003). Therefore the property of behaviour of ships in parametric rolling resonance in head waves has not been clarified thoroughly.

In order to establish appropriate safety measures against severe parametric rolling in head wave condition, influence of hull forms, operating condition (ship speed and course in waves), and wave condition (wave length and wave height) on the occurrence of parametric rolling resonance and the resultant magnitude of roll motion should be clarified.

In this context an experiment with a scale model of a post-Panamax containership was carried out in regular head waves at the 80 metres square basin of NMRI. As a result, some property of the head wave parametric rolling resonance, e.g. conditions in which the phenomenon is likely to occur, have been clarified. In order to examine the property of parametric rolling resonance, some numerical investigation was also carried out.

2. OUTLINE OF MODEL EXPERIMENT

The experiment was carried out with a free running model in regular waves of various length and height. Using an autopilot device and a motor controller, the encounter angle and the propeller revolution were kept constant for each run.

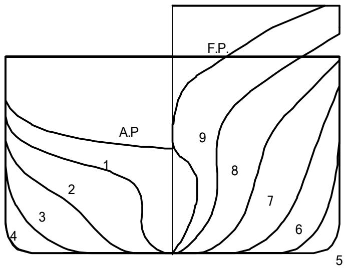

Figure 1 Body plan of model ship.

Table1. Principal particulars

	Ship	Model
Lpp (m)	283.8	3.700
B (m)	42.8	0.558
D (m)	24.4	0.318
d (m)	14.0	0.183
V (m^3)	106,970	0.237
Cb	0.629	0.629
GM (m)	1.08	0.014
T_ϕ (sec.)	30.26	3.460

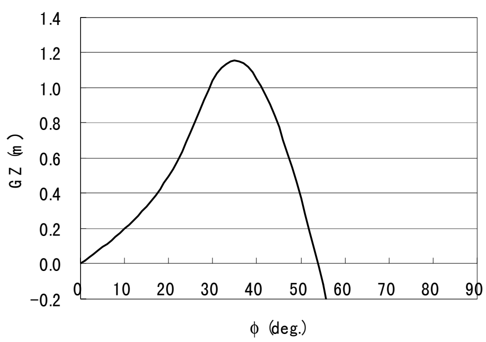

Figure 2 Stability curve (GM = 1.08 m).

The model ship is a 1/76.7 scale model of a 6600TEU containership. The main hull up to the upper deck and the forecastle were reproduced in the model, but the deckhouse was ignored. Figure 1 shows the body plan of the model and its principal particulars are shown in Table 1. Figure 2 shows the stability curve in the test condition, which was calculated with only the main hull and the forecastle taken into account.

In the experiment six degrees of freedom motion, relative water heights at stem, S.S.5 (weather side) and A.E., lateral acceleration beneath the upper deck at S.S.8, rudder angle, number of propeller revolution and speed and trajectory of the model were measured.

In order to investigate the overall property of parametric rolling resonance, the wavelength λ, the wave height Hw, the model speed Vm, and the encounter angle χ were varied. Table 2 summaries the length and height of waves used in the experiment. The wave height of 11 cm in the model scale corresponds to that of 8.4 m in the actual scale. The encounter angle was varied at every 15 degrees from 135 degrees (bow wave) to 180 degrees (pure head wave). The model speed was varied in a wide range so that the critical condition for parametric rolling resonance could be clarified.

Table2. Waves used in the experiment

	Hw				
λ/L	5cm	8cm	11cm	15cm	20cm
0.9			○		
1.0			○	○	
1.2		○	○	○	○
1.4			○		
1.6	○	○	○		
1.8			○		
2.0			○		
2.2			○		
2.4			○		

3. EXPERIMENTAL RESULTS

3.1 Examples of Parametric Rolling

Typical time series of the ship motion and the lateral acceleration at bow in parametric rolling resonance are shown in Figures 3 and 4.

Figure 3 shows the measured roll angle ϕ (top), pitch angle θ (middle) and lateral acceleration at bow $\ddot{\eta}$ (bottom) under the conditions of the wavelength to the ship length ratio $\lambda/L = 1.6$, the wave height Hw = 11 cm, the encounter angle $\chi = 180$ degrees, and the model speed Vm = 0.48 m/s (the corresponding Froude number Fn = 0.08). The ratio of the measured encounter period T_e to the natural rolling period T_ϕ, T_e/T_ϕ is about 0.48. Parametric rolling resonance, where there are two pitch cycles for each one roll cycle, occurs from the beginning. The roll motion immediately becomes in steady state where the amplitude of parametric rolling reaches 19 degrees. And the steady state amplitude of the lateral acceleration beneath the upper deck at S.S.8 is about 0.29 g (including the gravity component).

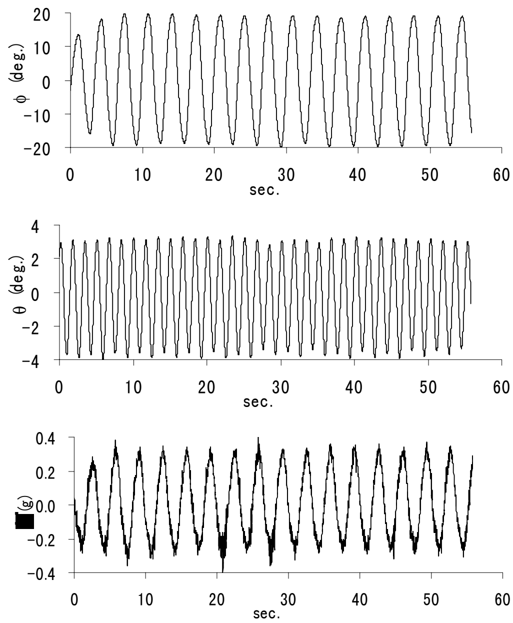

Figure 3 Measured roll angle (top), pitch angle (middle) and lateral acceleration at bow (bottom). $\lambda/L = 1.6$, Hw = 11 cm, $\chi = 180^\circ$, and Vm = 0.48 m/s (Fn = 0.08).

Time histories of the measured data under the conditions of $\lambda/L = 1.6$, Hw = 8 cm, $\chi = 135$ degrees, and Vm = 0.63 m/s (Fn = 0.11) are shown in Figure 4. In this case T_e/T_ϕ is about 0.49. At the beginning the model exhibits a large and small roll responses to every two encounter waves and gradually transits to parametric rolling response. But even at the end of the run, the rolling amplitude seems not to reach steady state.

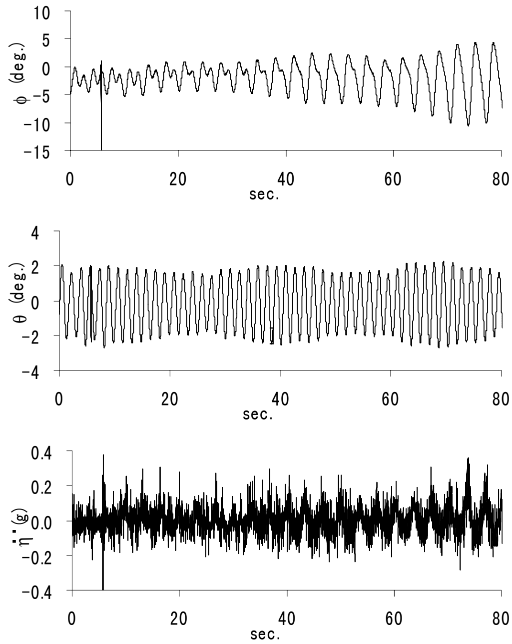

Figure 4 Measured roll angle (top), pitch angle (middle) and lateral acceleration at bow (bottom). $\lambda/L = 1.6$, Hw = 8 cm, $\chi = 135^\circ$, and Vm = 0.63 m/s (Fn = 0.11).

3.2 Occurrence of Parametric Rolling

Occurrence of parametric rolling resonance in waves of Hw = 11 cm are summarised in Figures 5 and 6.

Figure 5 shows the occurrence of parametric rolling resonance with the wavelength to the ship length ratio λ/L as parameter, where the encounter angle $\chi = 180$ degrees for the upper figure and $\chi = 150$ degrees for the lower one. The horizontal axis is the model speed in Froude number and the vertical axis is the ratio between the encounter period and the natural rolling period in each figure.

The experimental results are indicated on the lines that show the relation between the model ship speed and the encounter period. The symbol of black circle means condition where the steady state parametric rolling resonance (see Figure 3) was observed, the cross means one where parametric rolling resonance was not observed, and the white triangle means one where parametric rolling resonance was observed but did not reach the steady state (see Figure 4).

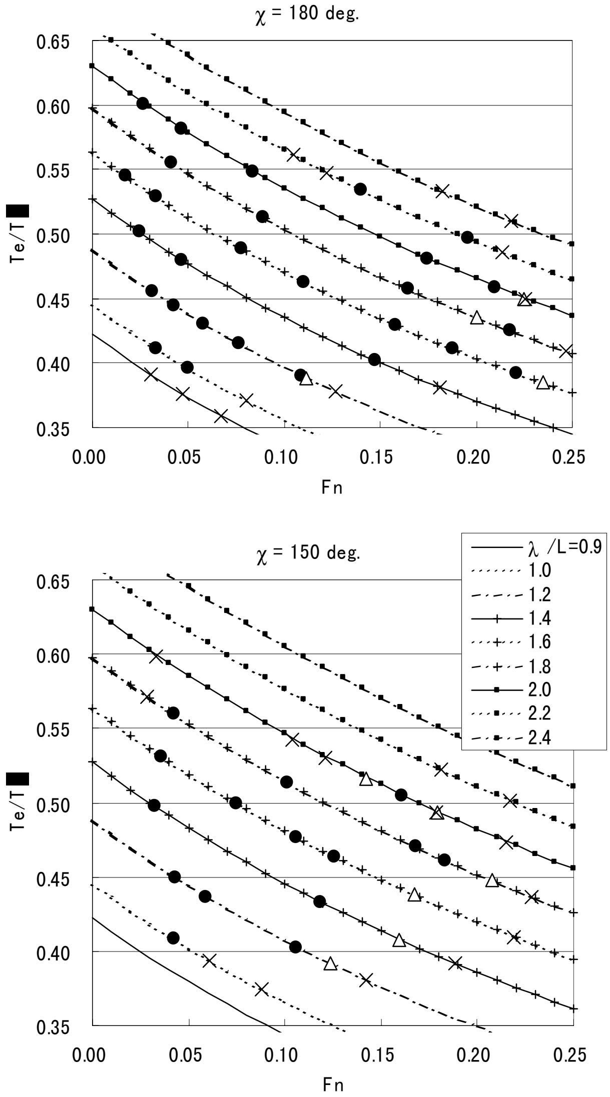

Figure 5 Occurrence of parametric rolling resonance. Hw = 11 cm and $\chi = 180^\circ$ (upper), $\chi = 150^\circ$ (lower).

Figure 6 summaries the occurrence of parametric rolling resonance at various encounter angels ($\chi = 135^\circ$, 150°, 165°, and 180°), where $\lambda/L = 1.2$ in the upper figure and $\lambda/L = 1.6$ in the lower one. In each figure the horizontal axis is the encounter angle and the vertical axis is the model speed in Froude number. Symbols mean as the same as in Figure 5.

From these figures we see the followings.

(1) Parametric rolling resonance occurs in relatively wide range of the encounter period to the natural rolling period ratio, T_e/T_ϕ, namely $T_e/T_\phi = 0.4 \sim 0.6$.

(2) In the same waves parametric rolling resonance is more likely to occur in pure head wave condition (χ = 180 degrees) than in bow wave condition (χ = 135 ~ 165 degrees).

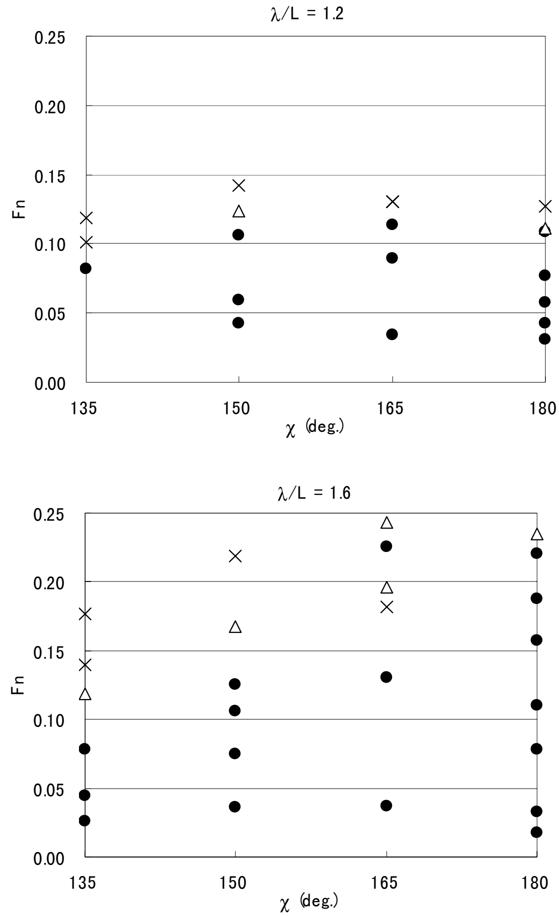

Figure 6 Occurrence of parametric rolling resonance. Hw = 11 cm and $\lambda/L = 1.2$ (upper), $\lambda/L = 1.6$ (lower).

3.3 Amplitude of Parametric Rolling

Influence of Encounter Period Figure 7 shows the steady state amplitude of parametric rolling for various encounter periods under the condition of the wave height Hw = 11cm and the encounter angle χ = 180 degrees. The horizontal axis is the encounter period to the natural rolling period ratio and the vertical axis is the parametric rolling amplitude ϕ_s normalised by the wave slope, ϕ_s/kHw (k is the wave number).

From this figure we see the followings.

(1) The amplitude of parametric rolling changes largely with the variation of the encounter period.
(2) For waves of the same length the parametric rolling amplitude becomes the maximum at about $T_e/T_\phi = 0.43 \sim 0.48$.
(3) The normalised rolling amplitudes for the same encounter period are almost the same except for waves of λ/L = 2.0 and 2.2.

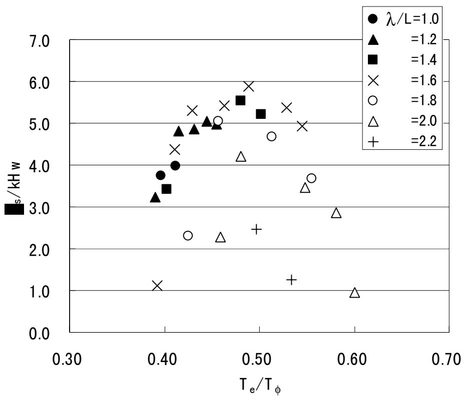

Figure 7 Influence of encounter period on parametric rolling amplitude. Hw = 11 cm and $\chi = 180°$.

Influence of Wave Height and Encounter Angle As indicated in Table 2, for waves of λ/L = 1.0, 1.2, and 1.6 measurements with different wave heights were carried out.

Figure 8 shows the steady state parametric rolling amplitudes measured under the conditions of χ = 180 degrees and $T_e/T_\phi = 0.40$ for λ/L = 1.0, $T_e/T_\phi = 0.45$ for λ/L = 1.2 and 1.6. The horizontal axis is the wave steepness Hw/λ, and the vertical axis is the normalised rolling angle. In the experiment the rolling amplitude did not become larger as the wave height increased beyond 11 cm. Therefore as indicated in Figure 8 the normalised rolling amplitude becomes smaller as the wave height increases.

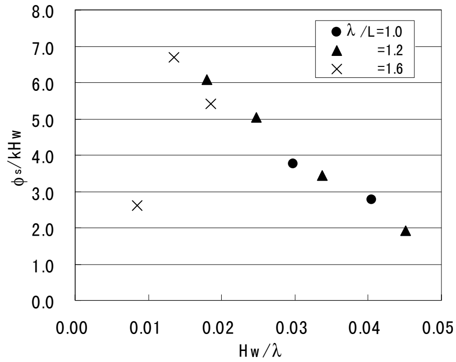

Figure 8 Influence of wave height on parametric rolling amplitude. $\chi = 180°$ and $T_e/T_\phi = 0.40$ for λ/L = 1.0, $T_e/T_\phi = 0.45$ for λ/L = 1.2 and 1.6.

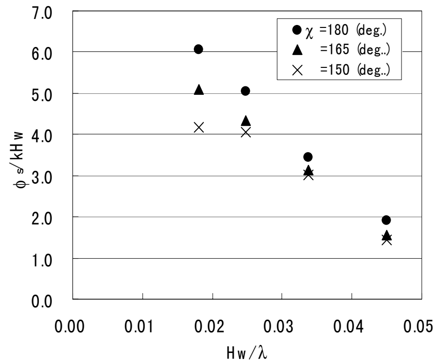

Figure 9 Influence of encounter angle on parametric rolling amplitude. λ/L = 1.2 and $T_e/T_\phi = 0.45$.

Figure 9 shows the influence of the encounter angle on the parametric rolling amplitudes under the conditions of $T_e/T_\phi = 0.45$ and λ/L = 1.2. The normalised rolling amplitudes for bow wave condition (χ =150 and 165 degrees) also become smaller as the wave height increases. And the rolling amplitudes for bow wave conditions are smaller than that for pure head wave condition (χ = 180 degrees).

Investigation into the influence of the wave height on the parametric rolling amplitude is important for judging whether a parametric rolling resonance leads to capsizing in severe waves. In order to draw conclusion of this issue it seems that more data in various condition (encounter period, wavelength wave height) is necessary.

4. NUMERICAL INVESTIGATION

In order to investigate the property of parametric rolling resonance further, we carried out numerical simulations with an equation of roll motion of a ship with stability variation in waves. In this paper, as the first step of the numerical investigation, we examine the parametric rolling resonance in pure head waves, where no roll exciting moment acts, and investigate effects of ship speed and wave height on the occurrence of parametric rolling resonance and the resultant rolling amplitude.

4.1 Equation of Roll Motion

Roll motion of a ship with stability variation in pure head wave can be generally expressed with equation (1).

$$\left(I_{xx}+J_{xx}\right)\ddot{\phi}+A\dot{\phi}+B\left|\dot{\phi}\right|\dot{\phi}+W\cdot GZ\left(\phi;t\right)=0 \qquad (1)$$

where ϕ is the roll angle, I_{xx} is the moment of inertia, J_{xx} is the added moment of inertia, A and B are the linear and the quadratic damping coefficients, W is the displacement, $GZ(\phi;\, t)$ is the time dependent restoring arm in waves. The dots over the symbol represent differentiation with respect to time t. By dividing all terms in equation (1) by (I_{xx} + J_{xx}), this equation is rewritten to following form.

$$\ddot{\phi}+2\alpha\dot{\phi}+\beta\left|\dot{\phi}\right|\dot{\phi}+\omega^{2}\frac{GZ\left(\phi;t\right)}{GM}=0 \qquad (2)$$

where GM is the metacentric height in still water, $\alpha = A/2(I_{xx}+J_{xx})$, $\beta = B/(I_{xx}+J_{xx})$, and ω^2 = WGM/(I_{xx} + J_{xx}). The stability variation in waves arises from the relative position of ship to wave $\xi_G(t)$, and the vertical ship motions, heave $\zeta(t)$ and pitch $\theta(t)$ in waves. Therefore the time dependent restoring arm in waves can be expressed as equation (3).

$$GZ\left(\phi;t\right)=GZ\left\{\phi;\ \xi_{G}(t),\zeta(t),\theta(t)\right\} \qquad (3)$$

GZ is calculated by integrating the hydrostatic pressure over the instantaneous submerged hull under the undisturbed wave profile, which is determined by the relative position of ship to wave and heave and pitch motions. With this calculation method the instantaneous variation of displacement due to the vertical motions is included. In this paper, the vertical motions are assumed to be linear to the wave height and computed with the strip theory.

In equation (2), the linear and the quadratic damping coefficients obtained from roll decay tests with forward velocity were used. Moreover we examine only steady state response of equation (2). Therefore numerical investigation was carried out with calculation method for obtaining bifurcation diagrams (Taguchi et al., 2003).

4.2 Occurrence of Parametric Rolling

Occurrence of parametric rolling resonance is directly detected with bifurcation diagram.

Influence of Encounter Period To draw bifurcation diagrams, numerical simulations were conducted for λ/L = 1.2, 1.6, and 2.0 with the ship speed gradually changed from Fn = 0 to 0.25 (service speed) but the wave height kept constant as Hw = 11 cm. Figure 10 shows the obtained bifurcation diagrams expressed as the function of the resultant encounter period to the natural rolling period ratio, T_e/T_ϕ. In the diagrams the normalised steady state roll responses at Poincaré section, $\phi(nT)/kHw$, are plotted as much as 20 cycles for every T_e/T_ϕ calculated. Two points at one T_e/T_ϕ means that parametric rolling resonance occurs at such encounter period. In each diagram experimental results are also shown with symbols of the same meaning as in Figure 5.

From the top diagram, it is found that for λ/L = 1.2 the numerical simulation predicts that parametric rolling resonance occurs in wide range of the encounter period to the natural rolling period ratio, namely T_e/T_ϕ = 0.32 (Fn= 0.23) ~ 0.49 (Fn = 0). However as indicated in the diagram, in the model experiment parametric rolling resonance was not observed at T_e/T_ϕ = 0.38. So the numerical simulation with equation (2) overestimates occurrence of parametric rolling resonance in short encounter period range.

For λ/L = 1.6 (the middle diagram) it is found that parametric rolling resonance occurs in all the calculated range of parameter. In this case good agreement between the numerical simulation and the experimental results is found.

For λ/L = 2.0 (the bottom diagram) the parametric rolling resonance is predicted to occur in the range of T_e/T_ϕ = 0.45 ~ 0.57. Compared with the experimental results, it is found that the numerical simulation well predicts the lower limit of the encounter periods for the occurrence of parametric rolling resonance, while it underestimates the upper limit.

The discrepancies between the numerical simulation and the experimental results in the range of encounter period which leads to parametric rolling resonance for λ/L = 1.2 and 2.0 seem to be mainly caused by the prediction of the stability variation in waves.

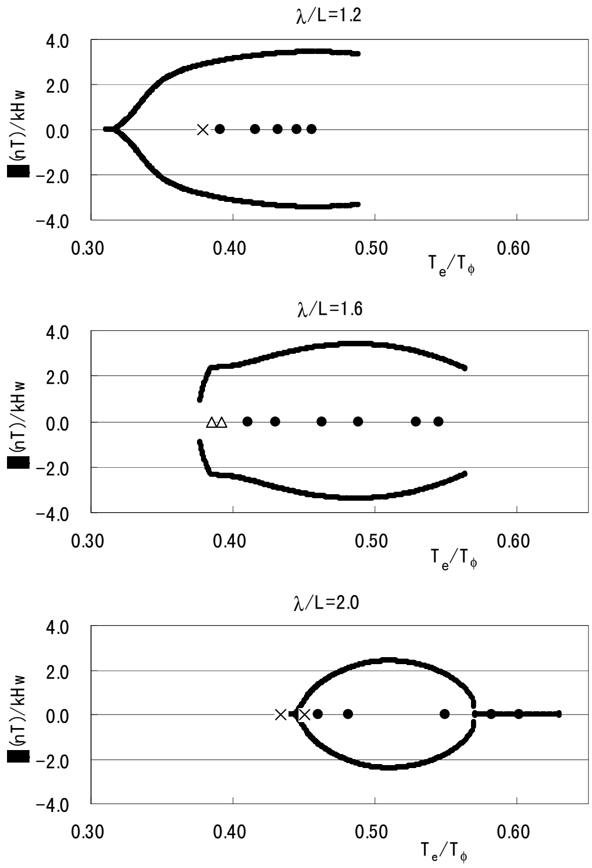

Figure 10 Bifurcation diagram with changing T_e/T_ϕ. Hw = 11 cm, $\chi = 180^\circ$, and λ/L = 1.2 (top); λ/L = 1.6 (middle); λ/L = 2.0 (bottom).

<u>Influence of Wave Height</u> Figure 11 shows bifurcation diagrams for λ/L = 1.2, 1.6, and 2.0 with the wave height gradually changed but the ship speed kept constant as the resultant encounter period satisfies that T_e/T_ϕ = 0.45. In each diagrams the horizontal axis is the wave steepness, while the vertical axis is the roll responses at Poincaré section normalised by the wave slope. The experimental results are also shown with the same manner as in Figure 10.

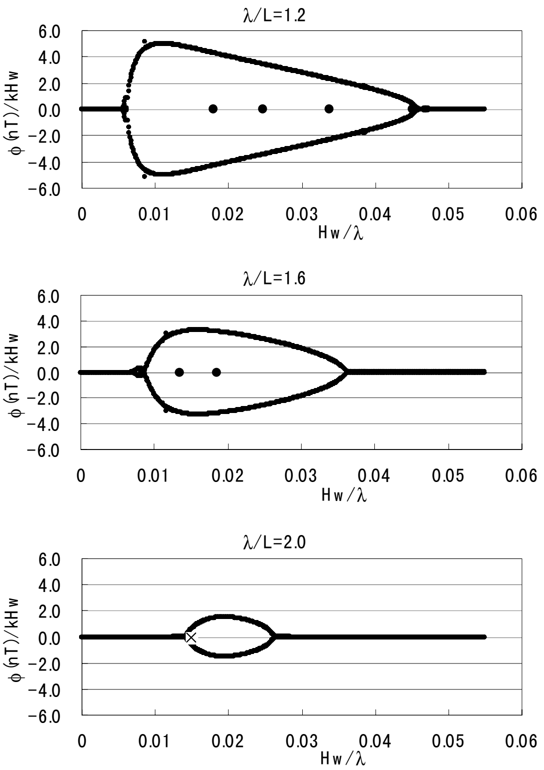

Figure 11 Bifurcation diagram with changing Hw/λ. T_e/T_ϕ = 0.45, χ = 180°, and λ/L = 1.2 (top); λ/L = 1.6 (middle); λ/L = 2.0 (bottom).

From Figure 11 it is found that the numerical simulations are almost consistent with the experimental results for all the wavelengths examined. And it is also found by the numerical simulations that there are two threshold wave heights, the lower limit and the higher limit of wave heights, for occurrence of parametric rolling resonance. For λ/L = 1.2 (the upper diagram), the numerical simulation predicts that as the wave height increases from 0, the parametric rolling resonance appears at about Hw/λ = 0.006 and continue to exist up to about Hw/λ = 0.045. As the wave height increases further, the parametric rolling resonance disappears. As shown in Figure 8, for λ/L = 1.2 the model experiment was carried out in waves of up to 20 cm in height (Hw/λ = 0.045), and parametric rolling resonance was observed in all the wave height tested. In order to confirm the existence of the higher threshold of wave height for parametric rolling resonance, additional model experiment in higher waves seems necessary.

Figure 11 also shows that as the wavelength increases, the range of wave height, which leads to parametric rolling resonance, becomes smaller. As the occurrence of parametric rolling is directly related to the stability variation in waves, further investigation including quantitative examination of the stability variation seems necessary to confirm the effects of the wave height on the occurrence of parametric rolling resonance.

4.3 Amplitude of Parametric Rolling

In this sub section, steady state parametric rolling amplitudes obtained in the calculation of bifurcation diagrams are examined.

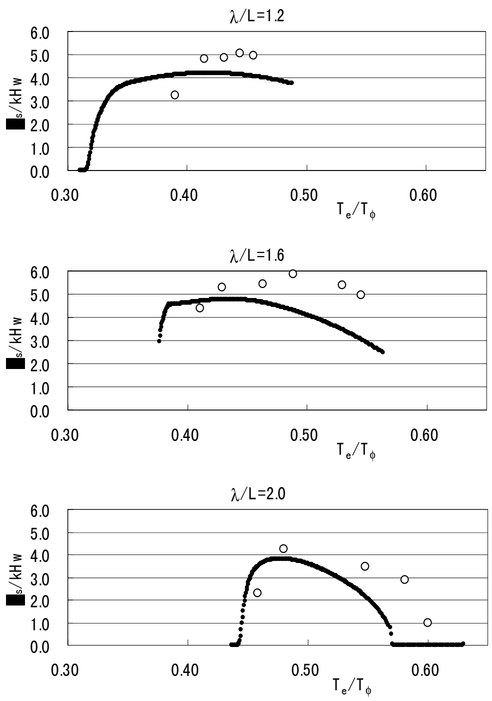

Figure 12 Influence of encounter period on parametric rolling amplitude. Hw = 11 cm, χ = 180°, and λ/L = 1.2 (top); λ/L = 1.6 (middle); λ/L = 2.0 (bottom).

<u>Influence of Encounter Period</u> Figure 12 shows the parametric rolling amplitude predicted by the numerical simulations with changing the ship speed as parameter. This figure corresponds to Figure 10. The horizontal axis is the encounter period to the natural rolling period ratio and the vertical axis is the steady state rolling amplitude normalised by

the wave slope. In the diagrams the experimental results are shown with the white circles.

From Figure 12 the numerical simulation seems to capture the tendency of parametric rolling amplitude found in the model experiment. But except for λ/L = 2.0, the numerical simulation underestimates the maximum amplitude of parametric rolling and there is also some discrepancy in the encounter period leading to the maximum response. As the stability curve of this ship is hard spring type (see Figure 2), the natural rolling period for large rolling amplitude tends to become shorter than that for small amplitude rolling. The numerical simulation may overestimate this effect and the resultant peak encounter period to the natural rolling period ratio becomes smaller than that in the model experiment.

Influence of Wave Height Figure 13 shows the predicted parametric rolling amplitude with changing the wave height as parameter. Compared to the experimental results, which are shown with white circles in the diagrams, the numerical simulation is found to predict the parametric rolling amplitude well. It is also found that the numerical simulation reproduces the tendency shown in the model experiment that the normalised parametric rolling amplitude becomes smaller as the wave height gets larger. In the numerical investigation, as shown in Figure 14, this tendency was observed at different encounter periods too.

5. CONCLUSIONS

The behaviour of a ship in parametric roll resonance in head waves was investigated experimentally with the free running model of a post-Panamax containership in regular waves. And some numerical investigation using an equation of roll motion of a ship with stability variation in waves was also carried out to examine the property of parametric rolling resonance.

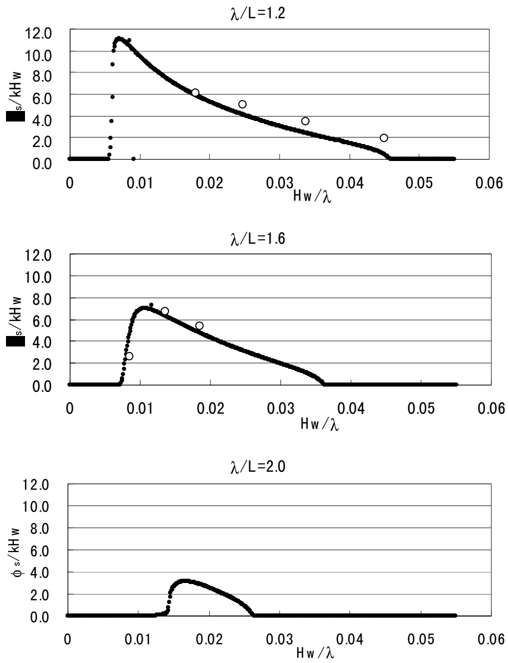

Figure 13 Influence of wave height on parametric rolling amplitude. $T_e/T_\phi = 0.45$, $\chi = 180^\circ$, and λ/L = 1.2 (top); λ/L = 1.6 (middle); λ/L = 2.0 (bottom).

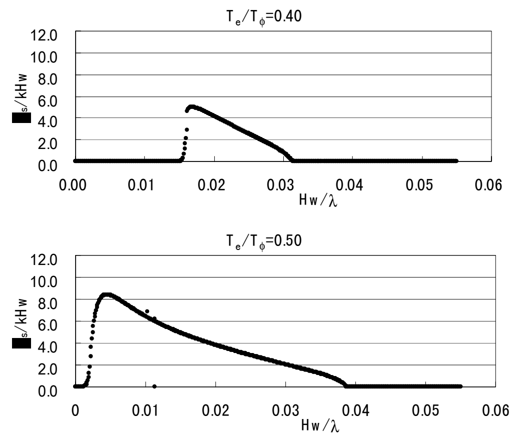

Figure 14 Influence of wave height on parametric rolling amplitude at $T_e/T_\phi = 0.40$ (upper) and 0.50 (lower). $\chi = 180^\circ$ and λ/L = 1.6.

As a result the followings are clarified.

(1) The parametric rolling resonance occurs in relatively wide range of the encounter period, where the ratio of it to the natural roll period, T_e/T_ϕ ranges from about 0.4 to

0.6.

(2) In the same wave parametric rolling resonance is more likely to occur in head wave condition (χ = 180 degrees) than in bow wave condition (χ = 135 ~ 165 degrees).

(3) The amplitude of parametric rolling changes largely with the variation of the encounter period and it becomes the maximum at about $T_e/T_\phi = 0.43 \sim 0.48$.

(4) The parametric rolling amplitude normalised by the wave slope becomes smaller as the wave height increases.

(5) The parametric rolling amplitudes for bow wave conditions become smaller than that for the head wave condition.

(6) The numerical simulation using equation (2) can predict the property of parametric rolling resonance qualitatively.

(7) Discrepancies found in both the occurrence range and the resultant amplitude of parametric rolling implies that some refinement for the stability variation model in waves, equation (3), is necessary to get more precise prediction.

6. ACKNOWLEDMENTS

Some parts of this investigation were carried out as a research activity of the SPL research panel of the Japan Ship Technology Research Association, funded by the Nippon Foundation. The authors express their sincere gratitude to the both organizations.

7. REFERENCES

Bulian, G., Francescutto, A., and Lugni, C., 2003, "On the Nonlinear Modeling of Parametric Rolling in regular and Irregular Waves", Proceedings of the 8th International Conference on the Stability of Ships and Ocean Vehicles, pp.305-323.

Dallinga, R.P., Blok, J.J., and Luth, H.R., 1998, "Excessive Rolling of Cruise Ships in Head and Following Waves", Proceedings of RINA International Conference on Ship Motions & Manoeuvrability, London, pp.1-16.

France, W.N., Levadou, M., and Treakle, T., 2003, "An Investigation of Head-Sea Parametric Rolling and Its Influence on Container Lashing Systems", Marine Technology, Vol. 40, No. 1, pp.1-19.

Neves, M.A.S. and Valerio, L., 2000, "Parametric Resonance in Waves of Arbitary Heading", Proceedings of the 7th International Conference on the Stability of Ships and Ocean Vehicles, pp.680-687.

Neves, M.A.S., Perez, N., and Lorca, O., 2003, "Analysis of Roll Motion and Stability of a Fishing Vessel in Head Seas", Ocean Engineering, Vol.30, pp.921-935.

Taguchi, H., Sawada, H., and Tanizawa, K., 2003, "A Study on Complicated Roll Motion of a Ship Equipped with an Anti-Rolling Tank", Proceedings of the 8th International Conference on the Stability of Ships and Ocean Vehicles, pp.607-616.